Generalized Pairing in Light Nuclei. II. Solution of the Hartree-Fock-Bogoliubov Equations with Realistic Forces and Comparison of Different Approximations*

A. L. Goodman†
Lawrence Radiation Laboratory, University of California, Berkeley, California 94720

and

G. L. Struble
Lawrence Radiation Laboratory and Department of Chemistry, University of California, Berkeley, California 94720

and

J. Bar-Touv
Lawrence Radiation Laboratory, University of California, Berkeley, California 94720, and Ohio State University, Columbus, Ohio 43210

and

A. Goswami
University of Oregon, Eugene, Oregon 94703
(Received 23 January 1970)

The Hartree-Fock-Bogoliubov (HFB) equations with generalized isospin pairing are numerically solved without any approximations, except imposing certain self-consistent symmetries. Realistic forces are used to make definite conclusions concerning the shapes of nuclei and the existence of isospin pairing. Comparison with previous approximations shows that in the s-d shell the HFB equations may not be quantitatively approximated by HF + BCS, HB − BCS, or by iterating between HF and BCS. Isospin pairing offers an explanation for axial symmetry in ^{24}Mg and ^{32}S and for the existence of low-lying vibrational states in ^{36}Ar.

I. INTRODUCTION

Nuclei in the first half of the s-d shell exhibit rotational features such as energy level spacings which obey an $I(I+1)$ law and enhanced electromagnetic transition probabilities between states within a rotational band. A very useful technique for calculating the wave functions of these states involves the construction of an intrinsic state, and the subsequent projection of angular momentum using the Hill-Wheeler integral[1] or various approximations based on the adiabatic nature of the rotational motion.[2] Intrinsic states have been calculated using deformed potential models[3] and, more recently, they have been calculated using Hartree-Fock (HF) theory. (A review of HF calculations in the s-d shell has been presented by Ripka.[4,5])

The HF description fails for the $N=Z$ even-even nuclei beyond ^{20}Ne. These failures have been discussed in detail in a previous publication[6] (hereafter referred to as I). However, to summarize the most important points of that discussion we note, (1) there are several experimental investigations which strongly indicate that the intrinsic shape of ^{24}Mg is prolate and axial while HF unambiguously predicts the shape to be triaxial, (2) for ^{28}Si, HF predicts both a low-lying oblate and an orthogonal low-lying prolate intrinsic state which is in contradiction to the experimental spectrum, (3) for ^{32}S, HF predicts a triaxial shape[7] with $\beta_2 = 0$ again in contradiction to the experimental spectrum, and (4) experiments suggest that ^{36}Ar can be interpreted phenomenologically as a vibrator, while HF predicts a well-deformed oblate intrinsic state giving low-energy rotational levels. Thus, if we are able to adopt the concept of an intrinsic state, then a more complicated one must be used.

In I we pointed out that the Hartree-Fock-Bogoliubov method (HFB) might be useful for describing the intrinsic states in the s-d shell. Recently, these calculations have been carried out by two groups[8,9] and they conclude that the usual $J=0$ pairing does not occur for $N=Z$ even-even nuclei. As clearly pointed out by Sauer, Faessler, and Wolter[9] and in I, this result should not be taken to mean that HFB will not produce new intrinsic states, since these authors have omitted neutron-proton correlations which have been shown to be important for $N=Z$ nuclei.[10] In I we solved the HFB equations including neutron-proton correlations using an approximation similar to that employed by Kumar and Baranger.[11] In this paper we solve the HFB equations exactly and make a careful examination of approximations which are usually employed in their solution. We also comment on the relevance of pairing in the intrinsic states

of the $N=Z$ even-even nuclei in the s-d shell. We use realistic interactions in this paper in order to make our conclusions about the existence of neutron-proton pairing and the shapes of these nuclei in a parameter-free manner. In Sec. II, we briefly develop the formulation of HFB, and discuss in some length the concept of self-consistent symmetry in HFB and the importance of the particular phases that we introduce. We also comment on the various approximations to HFB that have been used in discussing pairing. In Sec. III, we describe our calculations, attempt to justify the solutions, and discuss the effects of truncation and the imposition of self-consistent symmetries. In Sec. IV, we give the results of our calculations and discuss the validity of previous approximations. The implications of paired intrinsic states on the interpretation of experimental data in the s-d shell are discussed in Sec. V. In Sec. VI we present our conclusions.

II. SUMMARY OF HFB THEORY

Quasiparticle Transformation

We assume that a nucleus can be described by a two-body Hamiltonian

$$H=\sum_{\substack{ij\\ \mu\nu}}\langle i\mu|T|j\nu\rangle C^{\dagger}_{i\mu}C_{j\nu} + \tfrac{1}{4}\sum_{\substack{ijkl\\ \mu\nu\rho\delta}}\langle i\mu j\nu|V_a|k\rho l\delta\rangle C^{\dagger}_{i\mu}C^{\dagger}_{j\nu}C_{l\delta}C_{k\rho}\,, \tag{1}$$

where T is the kinetic energy and V is some effective two-nucleon interaction. Since we choose to work in an oscillator basis, $|i\tau\rangle$ denotes a wave function with quantum numbers $|n_i l_i j_i m_i \tau\rangle$. The Hamiltonian is next transformed to one written in terms of quasiparticles

$$a^{\dagger}_{\alpha\mu}=\sum_{i\nu}(u_{\alpha\mu,i\nu}C^{\dagger}_{i\nu}+v_{\alpha\mu,i\nu}C_{i\nu})\,, \tag{2}$$

where the $\mu_{\alpha\mu,i\nu}$ and $v_{\alpha\mu,i\nu}$ are complex coefficients of the HFB transformation. They are determined by requiring that the quasiparticles must be Fermions and that the Hamiltonian describes independent quasiparticles except for a residual interaction, i.e.,

$$H'=H-\lambda N=E'_0+\sum_{\alpha\mu}E_{\alpha\mu}a^{\dagger}_{\alpha\mu}a_{\alpha\mu}+H_{\rm INT}\,, \tag{3}$$

where

$$N=\sum_{i\nu}C^{\dagger}_{i\nu}C_{i\nu} \tag{4}$$

is the number operator, and $E_{\alpha\mu}$ are the quasiparticle energies. In the definition of λ,

$$\lambda=\lambda_p|p\rangle\langle p|+\lambda_n|n\rangle\langle n|\,, \tag{5}$$

p and n refer to the isospin indices for the proton and neutron, while λ_p and λ_n are Lagrange multipliers. H' and not H must be transformed, because when $H_{\rm INT}$ is neglected, the quasiparticle vacuum $|\Phi_0\rangle$ is an eigenstate of the independent-quasiparticle Hamiltonian but not of the neutron and proton number operators. The Lagrange multipliers are chosen so that

$$\langle N_p\rangle=Z,\quad \langle N_n\rangle=A-Z\,. \tag{6}$$

The part of H' which must be transformed to give the independent quasiparticles is written

$$H'_2=\sum_{\substack{ij\\ \mu\nu}}(\mathcal{H}-\lambda)_{i\mu,j\nu}:C^{\dagger}_{i\mu}C_{j\nu}: + \tfrac{1}{2}\sum_{\substack{ij\\ \mu\nu}}\Delta_{i\mu,j\nu}:C^{\dagger}_{i\mu}C^{\dagger}_{j\nu}: + \tfrac{1}{2}\sum_{\substack{ij\\ \mu\nu}}\Delta^{\dagger}_{i\mu,j\nu}:C_{i\mu}C_{j\nu}:\,, \tag{7}$$

where the normal order is taken with respect to the quasiparticle vacuum, and

$$\mathcal{H}_{i\mu,j\nu}=T_{i\mu,j\nu}+\Gamma_{i\mu,j\nu}\,, \tag{8}$$

$$\Gamma_{i\mu,j\nu}=\sum_{\substack{kl\\ \rho\sigma}}\langle i\mu k\rho|V_a|j\nu l\sigma\rangle\rho_{l\sigma,k\rho}\,, \tag{9}$$

$$\Delta_{i\mu,j\nu}=\tfrac{1}{2}\sum_{\substack{kl\\ \rho\sigma}}\langle i\mu j\nu|V_a|k\rho l\sigma\rangle t_{k\rho,l\sigma}\,. \tag{10}$$

ρ is the single-particle density matrix, and t is called the pairing tensor. They can be written in terms of the quasiparticle transformation

$$\rho_{i\mu,j\nu}\equiv\langle\Phi_0|C^{\dagger}_{j\nu}C_{i\mu}|\Phi_0\rangle=\sum_{\alpha\sigma}v_{\alpha\sigma,j\nu}v^{*}_{\alpha\sigma,i\mu}\,, \tag{11}$$

$$t_{i\mu,j\nu}\equiv\langle\Phi_0|C_{j\nu}C_{i\mu}|\Phi_0\rangle=\sum_{\alpha\sigma}u_{\alpha\sigma,j\nu}v^{*}_{\alpha\sigma,i\mu}\,. \tag{12}$$

The vacuum energy is given by

$$E_0=E_{\rm HF}+E_{\rm PAIR}\,,$$

where

$$E_{\rm HF}=\sum_{\substack{ij\\ \mu\nu}}(T-\lambda+\tfrac{1}{2}\Gamma)_{i\mu,j\nu}\rho_{j\nu,i\mu}+\lambda_p Z+\lambda_n(A-Z)\,,$$

and

$$E_{\rm PAIR}=\tfrac{1}{2}\sum_{\substack{ij\\ \mu\nu}}\Delta_{i\mu,j\nu}t^{\dagger}_{j\nu,i\mu}\,. \tag{13}$$

The coefficients in the transformation (2) and the quasiparticle energies are given by the solutions of the HFB equations

$$\begin{bmatrix} (\mathcal{H}-\lambda) & \Delta \\ \Delta^{\dagger} & (\lambda-\tilde{\mathcal{H}}) \end{bmatrix} \begin{bmatrix} u \\ v \end{bmatrix} = E \begin{bmatrix} u \\ v \end{bmatrix}. \tag{14}$$

The matrix to be diagonalized in (14) is often referred to as the κ matrix. Since the potentials depend on the solutions to the equations, the equations must be solved by iteration until self-consistency is achieved.

Self-Consistent Symmetries

The HFB equations contain both the HF and BCS equations as limits. The generalized BCS equations result from choosing an initial transformation having the form

$$a^{\dagger}_{i\mu} = \sum_{\nu} (u_{i\mu,i\nu} C^{\dagger}_{i\nu} + v_{i\mu,\bar{i}\nu} C_{\bar{i}\nu}), \tag{15}$$

where $|\bar{i}\rangle$ is the state time conjugate to $|i\rangle$, and $|i\rangle$ is some single-particle state chosen so that for any relevant set of isospin indices

$$\begin{aligned} &|\langle ij|V_a|i'j\rangle| \ll |\langle ij|V_a|ij\rangle| \\ &|\langle i\bar{i}'|V_a|j\bar{j}\rangle| \ll |\langle i\bar{i}|V_a|j\bar{j}\rangle|. \end{aligned} \tag{16}$$

The HFB equations may then be approximated by the usual 4×4 system of BCS equations.[10] It is, of course, not obvious *a priori* that such single-particle states can be found, and one of our important conclusions is that such approximations are not valid in the *s-d* shell. The HF equations can be obtained by simply choosing trial wave functions so that all $t_{ij}=0$ since from (10), $\Delta=0$. The structure of (14) insures that at each stage of the iteration, Δ remains zero so that the HFB equations converge to the HF solution.

This is an example of a symmetry which propagates through to the final self-consistent solution when it is initially built into the HFB equations. We will call these propagating symmetries (PS). It is important to consider such symmetries, because a seemingly arbitrary trial wave function might contain one or more of them, perhaps making it impossible to obtain the solution with the largest binding energy. Moreover the solution of a completely unrestricted HFB problem is impracticable even in the *s-d* shell. From (2) and (14) we see that this would involve diagonalizing 48×48 complex matrices until self-consistency is achieved. Thus it is imperative to use PS's to reduce the numerical problem. To this end we wish to specify a subset of the PS's which we will call self-consistent symmetries (SCS), and which can be uniquely defined. There are other PS's which, to our knowledge, can not be uniquely defined and which from time to time we have discovered numerically.

A SCS is defined as a unitary or antilinear unitary operator S which commutes with the H_2' part of the Hamiltonian [see (7)]. Sufficient conditions for such an operator to be a SCS are that:

(1) The total Hamiltonian (3) is invariant under the symmetry operation, i.e.,

$$[H', S] = 0. \tag{17}$$

(2) The trial wave functions are invariant up to a phase under the symmetry operations, i.e.,

$$S|\Phi_0\rangle = e^{i\phi}|\Phi_0\rangle. \tag{18}$$

(3) S maps the single-particle basis states into themselves.

The proof of this theorem and a rather complete discussion of SCS's has been recently given by Sauer.[13] If H_2' commutes with S, then, of course, the quasiparticle states $a^{\dagger}_{\alpha\mu}$ and $a^{\dagger}_{\alpha'\mu'} = S a^{\dagger}_{\alpha\mu} S^{-1}$ are degenerate, and may be specified by the labels of the irreducible representations of the symmetry group S. Thus, if we can show that our trial wave function satisfies conditions 1, 2, and 3 for some operator S, and if the matrix (14) is reduced to block form because of this symmetry, then, because we have a PS, we only need diagonalize the smaller blocks. Moreover with time reversal one only needs to solve one-half of the problem, since the time-conjugate states may be obtained from the relation

$$a^{\dagger}_{\bar{\alpha}\mu} = T a^{\dagger}_{\alpha\mu} T^{-1}. \tag{19}$$

For every SCS introduced, the generality of the theory is reduced, but often the dynamics of the problem suggest that such symmetries will be contained in the physically relevant HF or HFB solutions,[14] i.e., even if the SCS is broken in the trial wave function, it will be recovered at the end of the iteration process. We now list the SCS's used in this work and briefly discuss their implications.

Parity. The quasiparticles are labeled by the parity quantum number, and so the κ matrix is diagonalized separately in spaces of positive and negative parity. There can be no inversion-noninvariant deformations in the intrinsic state.

Time reversal. Use of this SCS allows one to

further decompose the κ matrix into blocks which define quasiparticles connected by time conjugation. In this paper we use harmonic-oscillator basis states and choose our phases so that

$$T|n\,l\,j\;m\;\tau\rangle=(-1)^{j-m+l}\,|n\,l\,j\;-m\;\tau\rangle.$$

Because T acts only on the space-spin coordinates, we will suppress the isospin coordinate for the discussion of time reversal. We divide the basis states into two sets, the first containing states with $m-\frac{1}{2}=$ an even integer and denoted by $|i\rangle$; the second contains those states having $m-\frac{1}{2}=$ an odd integer. They are chosen to be the time-conjugate states of the first set and are denoted by $|\bar{i}\,\rangle$. In this paper we restrict the pairing to be between time-conjugate states, i.e., we write the transformation (2) either with $u_{\alpha,i}$ and $v_{\alpha,\bar{i}}$, or $u_{\beta,\bar{i}}$ and $v_{\beta,i}$. Making this restriction in the trial wave functions breaks the κ matrix into blocks and introduces a PS. However, since we are dealing with even-even systems, we can choose time reversal as a SCS. This implies the restriction

$$a^{\dagger}_{\beta}=a^{\dagger}_{\bar{\alpha}}=T\,a^{\dagger}_{\alpha}\,T^{-1}, \tag{20}$$

which yields the relations

$$u_{\bar{\alpha},\bar{i}}=u^{*}_{\alpha,i}, \quad v_{\bar{\alpha},i}=-v^{*}_{\alpha,\bar{i}}, \tag{21}$$

and finally the HFB equations reduce to

$$\begin{pmatrix}\mathcal{H}-\lambda & \Delta\\ \Delta & \lambda-\mathcal{H}\end{pmatrix}\begin{pmatrix}u\\ v\end{pmatrix}=E\begin{pmatrix}u\\ v\end{pmatrix}, \tag{22}$$

where in contrast to (14) $\mathcal{H}=(\mathcal{H})_{ij}$, $\Delta=(\Delta)_{i\bar{j}}$, and both $\mathcal{H}$ and Δ are Hermitian.

Axial symmetry. This introduces a new quantum number Ω (the z projection of angular momentum) into the specification of the quasiparticle. This symmetry is introduced by restricting the quasiparticle transformations to states $|i\rangle$ with the same value of m, and states $|\bar{i}\rangle$ with $-m$. Although this symmetry is too restrictive[5] in HF (in ^{24}Mg and ^{32}S the lowest solutions are triaxial), it is one of the main purposes of this paper to examine whether this is still true in HFB.

Rotational symmetry. The quasiparticles are specified by the quantum numbers jm. This symmetry may be introduced by restricting the transformation so that the states $|i\rangle$ have the same jm, and the states $|\bar{i}\,\rangle$ have $j-m$. This symmetry is, in general, too restrictive, and in HF is valid only for doubly magic nuclei. We find within the framework of HFB that the lowest solutions in the s-d shell do not have this symmetry.

Rotations in Isospace. Since we have a general transformation which includes the coupling of neutrons and protons, there may be various SCS's in isospace. For example, we might demand rotational invariance, but this would restrict us to $N=Z$ nuclei and $T=0$ pairing. Since we limit ourselves to $N=Z$ even-even nuclei in this paper, this would be a possible symmetry. However we want to explore the possibility of lowering the energy by allowing nonconservation of isotopic spin in the intrinsic state. We might also demand rotational invariance about the z axis, but then we would restrict ourselves to neutron-proton pairing, and we wish to include neutron-neutron and proton-proton pairing as well. For $N=Z$ nuclei, it is physically reasonable to expect that the ground state has the property $\langle\vec{\mathbf{T}}\rangle=0$.[15] With this symmetry, the transformation in isospin space is written

$$\begin{pmatrix}a^{\dagger}_{1}\\ a^{\dagger}_{2}\\ \bar{a}_{1}\\ \bar{a}_{2}\end{pmatrix}=\begin{pmatrix}u_{1,1} & 0 & -v_{1,1} & -v_{1,2}\\ 0 & u_{1,1} & -v^{*}_{1,2} & v_{1,1}\\ v_{1,1} & v_{1,2} & u_{1,1} & 0\\ v^{*}_{1,2} & -v_{1,1} & 0 & u_{1,1}\end{pmatrix}\begin{pmatrix}C^{\dagger}_{p}\\ C^{\dagger}_{n}\\ \bar{C}_{p}\\ \bar{C}_{n}\end{pmatrix}, \tag{23}$$

and further, we choose the matrices $u_{1,1}$ and $v_{1,1}$ to be real. With this transformation, the pairing potential Δ may be written

$$\Delta=\begin{pmatrix}\Delta_{pp} & \Delta_{pn}\\ \Delta^{*}_{pn} & -\Delta_{pp}\end{pmatrix}, \tag{24}$$

where

$$\Delta_{pn}=\Delta^{T=1}_{pn}+i\Delta^{T=0}_{pn}. \tag{25}$$

A close examination of Δ shows that diagonal elements of $\Delta^{T=0}$ vanish if we choose the PS so that all coefficients are real (see Ref. 18). This result is independent of any SCS in isospace. Consequently, a complex HFB transformation is required for simultaneous $T=0$ and $T=1$ pairing.

In our discussion of time reversal, we showed that restricting the pairing to time-conjugate states gives time reversal as a SCS. This, however, excludes a possible mode of neutron-proton pairing where both particles are in the same space-spin state α and are coupled to $T=0$, i.e., we could consider $\alpha\alpha$ pairing in addition to the usual $\alpha\bar{\alpha}$ pairing. Such a mode could in principle be included in the general transformation. This would make the numerical calculation essentially impossible, since one loses the advantage of

breaking up the space into time-conjugate blocks (although the solution could still have time reversal as a SCS). Further, we no longer can have rotational invariance about the z axis as a SCS. In the next section we will calculate this mode and attempt to argue numerically that it is much less coherent than the usual mode. Therefore, it can be safely neglected. The lack of coherence of the $\alpha\alpha$-type of pairing can be explicitly demonstrated in the case of a simple $J=1$ force.[16]

Canonical Basis

In this subsection, we wish to describe several approximations to the most general HFB formalism and describe our method for presenting wave functions. This is done by use of a theorem similar to that of Bloch and Messiah[17] which states that the most general transformation B_{gen} is given by the product of three transformations[18]: (1) a transformation D in particle space which defines the canonical basis, and is obtained by diagonalizing the density matrix; (2) a generalized BCS transformation B_{sp}; and (3) a transformation R in the quasiparticle space,

$$B_{\text{gen}} = RB_{\text{sp}}D . \tag{26}$$

The well-known BCS approximation consists of assuming that we know *a priori* the canonical basis, and further that $\mathcal{H}$ and Δ are diagonal in the space-spin part of this basis. Then the κ matrix breaks into 4×4 blocks. If there is no neutron-proton pairing, the κ matrix further reduces to the familiar 2×2 matrices yielding the gap equation for the pairing of identical particles. In the HFB calculation of Baranger,[11] this simplification is achieved by use of the pairing-plus-quadrupole Hamiltonian. In this case, Δ is trivially diagonal in the HF representation of the $Q\cdot Q$ force. The approximation that we used in I was to take the coupled Hartree-Bogoliubov[19] and BCS equations which are equivalent to the HFB equations up to a unitary transformation, and note that if the off-diagonal elements of Δ are small, then they reduce to coupled generalized HF and BCS equations. Although this might intuitively seem a better approximation than BCS, it still depends on Δ being diagonal in the canonical basis. In any diagonal Δ approximation, R is the unit matrix. One of the major points to be explored in the present paper is the extent the nonzero off-diagonal elements of Δ affect the solution.

In Sec. IV we will discuss the various approximations numerically, and it will be useful to express the wave functions in terms of the three transformations. The first transformation is written as

$$C^{\dagger}_{r\mu} = \sum_{i\nu} D_{r\mu,i\nu}\, C^{\dagger}_{i\nu} . \tag{27}$$

The isospin structure of this transformation consistent with the SCS's is

$$D = \begin{bmatrix} D_{pp} & 0 \\ 0 & D_{nn} \end{bmatrix} , \tag{28}$$

where $D_{pp} = D_{nn}$. With our choice of SCS's, the second transformation B_{sp} may be written in terms of the submatrices

$$\begin{bmatrix} a^{\dagger}_{r1} \\ a^{\dagger}_{r2} \\ a_{\bar{r}1} \\ a_{\bar{r}2} \end{bmatrix} = \begin{bmatrix} u^{r}_{11} & 0 & -v^{r}_{11} & -v^{r}_{12} \\ 0 & u^{r}_{11} & -v^{r*}_{12} & v^{r}_{11} \\ v^{r}_{11} & v^{r}_{12} & u^{r}_{11} & 0 \\ v^{r*}_{12} & -v^{r}_{11} & 0 & u^{r}_{11} \end{bmatrix} \begin{bmatrix} C^{\dagger}_{rp} \\ C^{\dagger}_{rn} \\ C_{\bar{r}p} \\ C_{\bar{r}n} \end{bmatrix} , \tag{29}$$

where u^{r}_{11} and v^{r}_{11} are real numbers, and v^{r}_{12} is complex. The third transformation is written

$$a^{\dagger}_{\alpha\mu} = \sum_{r\nu} R_{\alpha\mu,r\nu}\, a^{\dagger}_{r\nu} , \tag{30}$$

and the isospin structure consistent with our SCS's becomes

$$R = \begin{bmatrix} R_{11} & 0 \\ 0 & R_{22} \end{bmatrix} , \tag{31}$$

where $R_{11} = R_{22}$. The general transformation can thus be specified by giving the real orthogonal matrices D_{pp} and R_{11}, and the coefficients u^{r}_{11}, v^{r}_{11}, and v^{r}_{12}. It is interesting that the canonical basis is doubly degenerate. Thus by taking appropriate[18] linear combinations of the degenerate solutions, it is possible to define the pairing between *two* single-particle states which become linear combinations of proton and neutron states with comple coefficients. These are the states which define the Bloch-Messiah canonical basis.[17] We do not use this mixed neutron-proton canonical basis, since it is inconvenient when comparing with previous results.

III. DESCRIPTION OF THE CALCULATION

A. Method of Solution

To solve the HFB equations (14) it is important

to have reliable initial guesses. In the first place, using completely random guesses may introduce undesirable PS's. In addition, such bad guesses may take a prohibitively long time to converge. We solve this problem in the following way:

(1) We first obtain various HF solutions. In particular, we find axially asymmetric, and both prolate and oblate axially symmetric solutions, and we often find several solutions that have the same shape. The HF single-particle states may be written as

$$C^{\dagger}_{\alpha\mu} = \sum_i D'_{\alpha\mu,i\mu} C^{\dagger}_{i\mu} . \tag{32}$$

(2) We next calculate the coefficients of a generalized BCS transformation

$$\begin{bmatrix} a^{\dagger}_{\alpha 1} \\ a^{\dagger}_{\alpha 2} \\ a_{\bar{\alpha}1} \\ a_{\bar{\alpha}2} \end{bmatrix} = \begin{bmatrix} u_\alpha & 0 & -v_\alpha & -v'_\alpha \\ 0 & u_\alpha & -v'^{*}_\alpha & v_\alpha \\ v_\alpha & v'_\alpha & u_\alpha & 0 \\ v'^{*}_\alpha & -v_\alpha & 0 & u_\alpha \end{bmatrix} \begin{bmatrix} C^{\dagger}_{\alpha p} \\ C^{\dagger}_{\alpha n} \\ C_{\bar{\alpha}p} \\ C_{\bar{\alpha}n} \end{bmatrix} , \tag{33}$$

where u_α and v_α are real, and v'_α is complex. The method of solving for the u's and v's has been given in an earlier paper.[10]

(3) The starting values of the HFB transformation coefficients are now given as

$$\begin{aligned} u_{\alpha\mu,i\nu} &= D'_{\alpha\mu,i\nu}\, u_\alpha\, \delta_{\mu,\nu} , \\ v_{\alpha 1,i1} &= -v_{\alpha 2,i2} = D'_{\alpha 1,i1} v_\alpha , \\ v_{\alpha 1,i2} &= v^{*}_{\alpha 2,i1} = D'_{\alpha 1,i1} v'_\alpha . \end{aligned} \tag{34}$$

(4) The starting value of λ is also obtained from solutions of the generalized BCS equations.[10]

(5) With these starting values, we obtain the final solutions by iteration until self-consistency is achieved.

Once the HFB transformation has been determined we express it as a product of the three Bloch-Messiah matrices which we discussed in Sec. II. The procedure for determining them is outlined below.

(1) The canonical basis is obtained by diagonalizing the density matrix (11). This gives us the transformation D of (27). We then determine ρ and t in the canonical basis.

(2) We now express ρ and t in terms of the coefficients of the second transformation $B_{\rm sp}$, [see (29)]. We then have the following relations:

$$\rho^{r}_{pp} = \rho^{r}_{nn} = v^{r\,2}_{11} + |v^{r}_{12}|^2 , \tag{35}$$

$$\rho^{r}_{pn} = \rho^{r}_{np} = 0 , \tag{36}$$

$$t^{r}_{pp} = u^{r}_{11} v^{r}_{11} = -t^{r}_{nn} , \tag{37}$$

$$t^{r}_{pn} = u^{r}_{11} v^{r\,*}_{12} = t^{r\,*}_{np} , \tag{38}$$

where $\rho^{r}_{\mu\nu} = \rho_{r\mu,r\nu}$ and $t^{r}_{\mu\nu} = t_{r\mu,\bar{r}\nu}$. u^{r}_{11} may be obtained from (35) as

$$|u^{r}_{11}| = (1 - \rho^{r}_{pp})^{1/2} . \tag{39}$$

We choose $u^{r}_{11} \geq 0$, and then v^{r}_{11} and v^{r}_{12} can be obtained from (37) and (38).

(3) Since $B_{\rm gen}$, D, and $B_{\rm sp}$ are now known, R can be determined from (26). Further details can be found in Ref. 18.

B. Choice of Force

In I, we used a Rosenfeld-Yukawa force in our calculations. Since the existence and importance of the isospin pairing correlations depend on the nature of the effective interaction (for example, the relative strength of $T=0$ versus $T=1$ matrix elements or the s-wave triplet to singlet strength), we have used three types of force in this work; the first two are commonly regarded as realistic. The rationale for using such forces in both the HF and HFB calculations is that these calculations are to be regarded as a caricature of an exact shell-model calculation in a sufficiently large model space.

(1) Yale t matrix. The Yale potential[20] was determined by very accurate fitting of the nucleon-nucleon scattering data. Since a hard core is included, one must replace the matrix elements of V by those of t. The t-matrix elements used in this paper are those calculated by Shakin, Waghmare, and Hull[21] from the Yale potential. As is customary, the dependence of the t matrix on the single-particle wave functions and energies (double self-consistency) is ignored. The shell-model space is confined to the lowest three oscillator shells. The oscillator parameter ($b = \sqrt{\hbar/m\omega}$) that we choose is $\sqrt{3.1}$ fm. This enables us to compare our results with previous HF calculations.[22]

(2) Nestor-Davies-Krieger-Baranger (NDKB) potential.[23] This potential was specifically designed with no hard core for Hartree-Fock calculations. The effect of the hard core is simulated by using a velocity-dependent term in the potential. In fitting the force parameters (we use set number 3), primary emphasis was given to reproducing the binding energy and equilibrium density of nuclear matter, so that the second-order

corrections to the binding energy are small.

(3) Rosenfeld-Yukawa effective interaction. This force has been widely used in the s-d shell (see discussion in I). For the HFB calculations we truncate to the $N=2$ oscillator shell, and replace the kinetic energy by single-particle energies (see I and Ref. 4). As in I, we use single-particle energies which correspond to the experimental ones found in ^{17}O (Rosenfeld 1) and also to energies which were used in the HF calculation[24] of ^{24}Mg (Rosenfeld 2). We use this force in order to make a comparison with the results in I, and so that in the future a comparison can be made with the results of exact shell-model calculations.

C. Validity of Number Nonconservation Approximations

In I we compared number nonconserving BCS with the results of exact number projection for $T=0$ pairing. Although we found that the total energies do not change appreciably, the pairing energy was reduced by approximately 30% in the number-conserving case. This was due to the drastic reduction of the dispersion of the particles across the Fermi surface (see Fig. 1 in I). For number nonconservation to be accurate, we would expect that the binding energy should vary linearly with N. Because of the dominance of n-p pairing, this linearity will be particularly important between odd-odd and even-even $N=Z$ nuclei. A cursory glance at the experimental mass symmetries of the s-d shell even-mass nuclei, shows the presence of a sharp discontinuity at the $N=Z$ even-even nuclei. For example, the mass discontinuity at ^{24}Mg is $\Delta M(^{24}\mathrm{Mg}) \equiv M(^{26}\mathrm{Al}) - 2M(^{24}\mathrm{Mg}) + M(^{22}\mathrm{Na}) = 10.5$ MeV. However, this experimental discontinuity is of no relevance in pairing theory. Rather it will be the discontinuity calculated with the underlying HF wave functions. It is interesting to note that with the triaxial HF solution calculated in Ref. 22, $\Delta M(^{24}\mathrm{Mg}) = 11.3$ MeV. This is caused by the presence of a large gap in the triaxial solution. In I it was shown that it is just this gap which prevents the (number-nonconserving) pairing field from building up in the triaxial HF basis. On the other hand, using the axially symmetric prolate HF solution given in Ref. 22, one obtains $\Delta M(^{24}\mathrm{Mg}) = -3.8$ MeV. Since the mass discontinuity is relatively small in this case, a strong number-nonconserving $T=0$ pair field builds up on this solution (see Secs. IV and I). However this discontinuity is large enough to severely limit the accuracy of the number-nonconserving BCS method. To our knowledge, a number-conserving HFB calculation has not been carried out. One can get a rough estimate of the validity of the number-nonconserving method by calculating the discontinuity for the canonical basis. Using the canonical basis functions given in Sec. IV, we find $\Delta M(^{24}\mathrm{Mg}) = -3.7$ MeV, $\Delta M(^{32}\mathrm{S}) = -7.1$ MeV, and $\Delta M(^{36}\mathrm{Ar}) = 5.0$ MeV. This suggests that the number-nonconserving method is not any more valid in HFB than in BCS.

D. Absence of α-α and $T=1$ Pairing

In Sec. II we pointed out that we have not included the possibility of α-α pairing in our calculations, but in I it has already been shown that a dominance of a pair field of one kind precludes the emergence of other pairing fields. For example, $T=1$ pairing is suppressed by the $T=0$ field for all $N=Z$ even-even nuclei. This remains true for the solutions presented in this paper. With the Yale force and a space of three oscillator shells we also investigated α-α pairing, and found ^{24}Mg has a binding energy of -130.53 MeV, while ^{32}S and ^{36}Ar have binding energies of -225.12 and -291.07 MeV, respectively. These solutions are obtained with the nuclei artificially constrained to be axially symmetric. When this constraint is removed, the nuclei either gain ~0.3 MeV in binding energy or fall into the triaxial HF solutions. For pure α-$\bar{\alpha}$ pairing, the binding energies for these nuclei are -132.53, -229.66, and -291.76 MeV. The relative lack of coherence of the α-α pair field is clear. It is therefore expected that this field will be suppressed by the stronger α-$\bar{\alpha}$ pair field in a more general calculation, although this has not yet been investigated numerically.

IV. NUMERICAL RESULTS

A. Comparison of the HF and Canonical Basis and the Validity of the Approximation Used in I.

In Table I we give the HFB wave functions for the solutions with the largest binding energy in terms of the three Bloch-Messiah transformations defined in Eqs. (26)–(31). These wave functions were obtained with the Yale t matrix using a basis of three oscillator shells. As pointed out in Sec. II, a measure of the deviation of our previous approximation from the complete HFB is given by the deviation of R from the unit matrix. It can be seen from Table I, that this deviation is appreciable for ^{24}Mg and ^{32}S, and is very large for ^{36}Ar. A similar measure can be obtained by comparing the HF wave functions D' given in Ref. 21 with the canonical wave functions D of Table V. Again large deviations are due to the fact that Δ is not diagonal in the canonical basis. In Table II we give the matrix Δ in the canonical basis for ^{24}Mg, ^{32}S, and ^{36}Ar. Not surprisingly, we find that Δ has large off-diagonal elements for all three nuclei. Although ^{24}Mg has large off-diagonal ele-

TABLE I. HFB wave functions for the lowest-energy nontrivial HFB solutions for ^{24}Mg, ^{32}S, and ^{36}Ar. Calculations are done with the Yale-Shakin potential in the s-p-s-d-shell basis. $\Omega\pi$ denotes the component of total angular momentum on the symmetry axis and the parity, respectively, for each orbital. E denotes the quasiparticle energies in MeV. The general quasiparticle transformation is displayed as a product of three transformations as explained in the text. In the column giving $[\mathrm{Im}v_{12}]^2$, the sign of $\mathrm{Im}v_{12}$ is given in the parenthesis. Note that $v_{11}=\mathrm{Re}v_{12}=0$ for all the solutions. λ is the Fermi energy.

$\Omega\pi$	E	Transformation R				$[\mathrm{Im}v_{12}]^2$	Transformation D			
						^{24}Mg ($\lambda=-9.150$ MeV)				
							$1d_{5/2}$			
$\frac{5}{2}+$	3.777				1.000	(+)0.034	1.000			
							$1d_{5/2}$	$1d_{3/2}$		
$-\frac{3}{2}+$	2.651			0.167	0.986	(+)0.008	0.347	−0.938		
	7.982			0.986	−0.167	(−)0.684	0.938	0.347		
							$1s_{1/2}$	$1d_{5/2}$	$2s_{1/2}$	$1d_{3/2}$
$\frac{1}{2}+$	2.158	0.247	0.923	−0.296	0.015	(+)0.014	0.143	−0.409	−0.747	0.504
	5.058	0.926	−0.134	0.351	−0.036	(−)0.317	0.024	−0.617	−0.175	−0.767
	6.503	0.285	−0.361	−0.888	0.021	(+)0.953	0.067	0.672	−0.622	−0.396
	49.655	0.024	−0.011	0.036	0.999	(+)1.000	0.987	0.029	0.155	−0.027
							$1p_{3/2}$			
$-\frac{3}{2}-$	19.334				1.000	(−)0.997	1.000			
							$1p_{3/2}$	$1p_{1/2}$		
$\frac{1}{2}-$	16.958			0.990	0.139	(−)0.996	0.570	0.821		
	26.094			−0.139	0.990	(+)0.998	0.821	−0.570		
						^{32}S ($\lambda=-14.245$ MeV)				
							$1d_{5/2}$			
$\frac{5}{2}+$	7.073				1.000	(−)0.981	1.000			
							$1d_{5/2}$	$1d_{3/2}$		
$-\frac{3}{2}+$	2.931			0.906	0.422	(+)0.527	0.712	0.702		
	5.337			0.422	−0.906	(−)0.949	0.702	−0.712		
							$1s_{1/2}$	$1d_{5/2}$	$2s_{1/2}$	$1d_{3/2}$
$\frac{1}{2}+$	3.238	0.322	0.937	−0.136	0.011	(−)0.107	0.106	0.487	−0.533	−0.684
	5.425	0.378	−0.260	−0.884	0.086	(+)0.480	0.039	0.643	−0.306	0.702
	6.468	0.868	−0.235	0.435	−0.052	(−)0.974	0.158	−0.591	−0.765	0.199
	55.521	0.010	−0.000	0.100	0.995	(−)0.999	0.981	0.017	0.193	0.014
							$1p_{3/2}$			
$-\frac{3}{2}-$	29.564				1.000	(+)0.997	1.000			
							$1p_{3/2}$	$1p_{1/2}$		
$\frac{1}{2}-$	21.848			0.998	0.068	(−)0.991	0.734	−0.680		
	28.358			0.068	−0.998	(+)0.996	0.680	0.734		
						^{36}Ar ($\lambda=-16.772$ MeV)				
							$1d_{5/2}$			
$\frac{5}{2}+$	8.012				1.000	(−)0.993	1.000			
							$1d_{5/2}$	$1d_{3/2}$		
$-\frac{3}{2}+$	2.488			0.830	0.557	(+)0.877	0.703	0.711		
	6.771			0.557	−0.830	(−)0.980	0.711	−0.703		
							$1s_{1/2}$	$1d_{5/2}$	$2s_{1/2}$	$1d_{3/2}$
$\frac{1}{2}+$	2.750	0.608	0.754	−0.249	0.003	(−)0.322	0.088	0.451	−0.528	−0.715
	4.927	0.793	−0.561	0.239	−0.022	(+)0.852	0.042	0.635	−0.368	0.678
	6.486	−0.041	0.343	0.938	−0.038	(−)0.988	0.105	−0.627	−0.752	0.173
	57.983	0.014	−0.002	0.042	0.999	(−)0.999	0.990	−0.000	0.142	0.017
							$1p_{3/2}$			
$-\frac{3}{2}-$	31.500				1.000	(+)0.998	1.000			
							$1p_{3/2}$	$1p_{1/2}$		
$\frac{1}{2}-$	26.044	0.964	0.267			(−)0.994	0.741	−0.671		
	30.354	0.267	−0.964			(+)0.998	0.671	0.741		

TABLE II. The $T=0$ pair potential (in MeV) in the canonical basis, corresponding to the solutions in Table I.

$\Omega\pi$	^{24}Mg				^{32}S				^{36}Ar			
$\frac{5}{2}+$	1.372				−1.934				−1.372			
$-\frac{3}{2}+$	1.428	0.678			3.355	0.466			2.508	0.425		
	0.678	−2.604			0.466	−2.166			0.425	−1.526		
$\frac{1}{2}+$	1.189	0.378	−0.116	1.058	−3.707	−0.365	−0.530	−0.402	−3.862	−0.553	−0.264	−0.610
	0.378	−2.589	0.845	−0.458	−0.365	3.561	−0.103	0.019	−0.553	−2.755	−0.256	0.039
	−0.116	0.845	2.547	0.367	−0.530	−0.103	−1.940	−0.989	−0.264	−0.256	−1.360	−0.310
	1.058	−0.458	0.367	1.656	−0.402	0.019	−0.989	−4.104	−0.610	0.039	−0.310	−4.016
$-\frac{3}{2}-$	−2.178				3.411				2.620			
$\frac{1}{2}-$	−2.264	−0.022			−4.153	−0.015			−4.003	−0.034		
	−0.022	2.537			−0.015	3.524			−0.034	2.707		

ments, the canonical basis is remarkably similar to the HF solution, and the dispersions calculated from the HFB and the diagonal Δ approximation of I are also very similar. Thus, for this particular case only the third transformation is effected by the nondiagonal elements of Δ. We know of no criteria that will tell *a priori* whether Δ will be diagonal in the canonical basis. Therefore we conclude that in the *s-d* shell the complete HFB is necessary, since the diagonal Δ approximation may be misleading. This is especially true for excited-state calculations which depend on quasiparticle energies and wave functions.

In Table III we compare E_{HF}, E_{PAIR}, and E_{TOTAL} for the HF + BCS approximation,[10] the diagonal Δ HFB approximation of I, and the complete HFB calculated for this paper. From this comparison, we conclude that HFB always gives the largest binding energy. Second, we observe that the pairing energy increases in the HFB (largely at the expense of HF energy) often by more than a factor of 2. This is understandable, because the HF wave functions were derived in order to maximize the HF binding energy. When the pairing field is allowed to build up simultaneously and self-consistently, it should be expected that the pair field will gain energy at the expense of the HF field.

TABLE III. A comparison of pairing theories. E_{HF}, E_{PAIR}, and E_{TOTAL} denote the Hartree-Fock, pairing, and the total energies in MeV.

Method	E_{HF}	E_{PAIR}	E_{TOTAL}
	^{24}Mg		
HF + BCS	−126.02	−6.31	−132.33
Approx. HFB	−126.53	−5.58	−132.11
HFB	−124.73	−7.80	−132.53
	^{32}S		
HF + BCS	−219.01	−4.75	−223.76
Approx. HFB	−218.94	−4.88	−223.83
HFB	−215.32	−9.21	−224.53
	^{36}Ar		
HF + BCS	−283.71	−3.39	−287.10
Approx. HFB	−282.76	−3.92	−286.68
HFB	−282.24	−9.52	−291.76

B. Physical Properties of the HFB Solutions

In Table IV, we list certain properties which describe the intrinsic states for all the paired HFB solutions we have obtained for all the $N=Z$ even-even *s-d* shell nuclei with all the forces we have discussed in Sec. III. The NDKB1 solutions were obtained in a space of three oscillator shells using the Nestor-Davies-Krieger-Baranger force. The NDKB2 solutions were obtained using the same force, but in a space expanded to include four oscillator shells. The parameters characterizing the HFB intrinsic states that we shall discuss are defined below. We specify the shape of an intrinsic state by giving its quadrupole and hexadecapole moments

$$Q_{20}=\langle\sum_{i=1}^{A} r_i^{\,2}\,Y_{20}(\Omega_i)\rangle$$

$$Q_{40}=\langle\sum_{i=1}^{A} r_i^{\,4}\,Y_{40}(\Omega_i)\rangle. \tag{40}$$

It is also usual to define the shape of a nucleus with the size-independent shape parameters β_2 and β_4 which for axially symmetric deformations are defined by

$$\beta_2=\tfrac{4}{5}\pi\,Q_{20}/R_2A \tag{41}$$

$$\beta_4=\tfrac{4}{7}\pi\,Q_{40}/R_4A, \tag{42}$$

where R_2 is taken to be the rms radius

$$R_2=\frac{1}{A}\left\langle\sum_{i=1}^{A} r_i^{\,2}\right\rangle, \tag{43}$$

TABLE IV. Paired HFB solution in the s-d shell. Only nontrivial solutions are displayed. In the third column denoting the shape of the HFB solution, the shape of the trial HF wave function is also shown in parenthesis: P: prolate, O: oblate, S: spherical. In case there is more than one HF solution of a given shape, they are distinguished by an additional member, e.g., P1, P2, etc. The numbers in the gap column are the sum of the two smallest quasiparticle energies.

Nucleus	Force	Shape	Mode	E_{PAIR}	E_{TOTAL}	Q_{20}	Q_{40}	Gap
^{20}Ne	Rosenfeld 2	Oblate (O)	$T=0$	−7.625	−41.697	−5.9	25.9	4.78
		Prolate (P2)	$T=0$	−6.587	−41.444	2.7	−53.5	4.76
	Yale	Prolate (S)	$T=0$	−2.324	−101.505	15.4	80.0	4.74
^{24}Mg	Rosenfeld 1	Prolate (P2)	$T=0$	−6.438	−77.526	15.6	−14.9	5.68
		Oblate (O1, O2)	$T=0$	−6.551	−77.238	−13.0	40.8	5.44
	Rosenfeld 2	Prolate (P1)	$T=0$	−4.576	−95.170	15.6	−0.5	5.20
		Oblate (O1, O2, O3)	$T=0$	−6.858	−93.865	−12.4	58.1	4.80
	Yale	Prolate (P)	$T=0$	−7.802	−132.527	19.0	−12.1	4.32
		Oblate (O1, O2)	$T=0$	−17.205	−132.049	−12.1	31.4	5.98
	NDKB 1	Prolate (P)	$T=0$	−8.121	−110.388	15.9	13.4	4.98
		Oblate (O)	$T=0$	−11.802	−109.301	−12.5	47.5	4.22
	NDKB 2	Prolate (P)	$T=0$	−9.637	−116.651	22.5	6.0	5.76
		Oblate (O)	$T=0$	−15.887	−114.131	−16.6	52.8	5.28
^{28}Si	Rosenfeld 1	Prolate (O2)	$T=0$	−7.234	−123.420	0.13	116.0	4.70
	Rosenfeld 2	Oblate (O2)	$T=0$	−2.207	−150.041	−0.5	−96.5	5.72
		Prolate (O3)	$T=0$	−6.050	−147.808	0.14	110.5	3.80
	NDKB 1	Prolate (P, S)	$T=0$	−9.933	−140.610	15.1	−20.9	3.76
		Prolate (O2)	$T=0$	−14.375	−138.733	3.1	−84.0	3.72
	NDKB 2	Prolate (O2, S)	$T=0$	−8.359	−146.853	24.9	−72.0	4.40
^{32}S	Rosenfeld 1	Oblate (O2, O3)	$T=0$	−5.835	−178.385	−1.3	−110.0	5.62
		Prolate (P)	$T=0$	−7.276	−178.179	6.5	−94.5	5.76
		Prolate (S)	$T=0$	−12.724	−176.173	3.4	37.9	4.74
	Rosenfeld 2	Oblate (O1, O3)	$T=0$	−1.385	−212.901	−1.5	−95.8	5.30
	Yale	Oblate (NDKB1-O)	$T=0$	−13.233	−229.658	−17.0	2.5	5.86
		Prolate (P)	$T=0$	−9.208	−224.531	13.6	−66.3	4.58
	NDKB 1	Oblate (O)	$T=0$	−6.988	−179.696	−15.5	5.9	3.24
		Prolate (P, S)	$T=0$	−6.031	−179.266	12.8	−38.2	3.94
	NDKB 2	Oblate (O)	$T=0$	−9.977	−183.910	−20.4	0.9	4.14
		Prolate (P, S)	$T=0$	−10.953	−183.153	16.8	−52.6	5.94
^{36}Ar	Rosenfeld 1	Prolate (P, S)	$T=0$	−7.722	−237.234	4.9	−26.3	4.36
	Rosenfeld 2	Prolate (P, S)	$T=0$	−5.079	−277.826	3.9	−21.5	3.74
	Yale	Oblate (P, S)	$T=0$	−9.523	−291.765	−11.3	−37.0	4.58
	NDKB 1	Prolate (P, S)	$T=0$	−5.904	−224.664	6.0	−17.7	2.72
	NDKB 2	Prolate (P)	$T=0$	−11.260	−226.519	7.5	−19.9	3.94

and

$$R_4=\frac{1}{A}\left\langle\sum_{i=1}^{A} r_i{}^4\right\rangle, \tag{44}$$

and A is the mass number. From Table IV, we conclude that HFB theory is less ambiguous than HF+BCS in the sense that as many as four different HF+BCS solutions converge to the same HFB solution. All of the forces lead to more or less the same conclusions about the physical properties of intrinsic states. Also, we observe that the energy gaps are, on the average, 20% larger in the HFB solutions compared with the HF+BCS approximation, which indicates an increased stability for these solutions. Finally we observe that increasing the shell space to include the next major shell has the property that deformation increases due to core polarization, reflected by a substantial increase (of approximately 40%) in β_2.

Also from Table IV one can see there is a definite tendency for the pairing energy to increase as one expands the shell-model space. The amount of increase is only 20% in ^{24}Mg, but increases to 90% in ^{36}Ar. The effective energy gap of two quasiparticle excitations displayed in the last column of Table IV increases from 20% in ^{24}Mg to 45% in the case of ^{36}Ar, which is due to the enlargement of the space. This demonstrates that the solutions become more stable as one enlarges the shell-model space.

The effect of various factors on the underlying

self-consistent field, such as the truncations of the shell space or the inclusion of pairing correlations, can be demonstrated in a pictorial manner by plotting the mass distribution defined by

$$\mu(\vec{r}) = \sum_{ij} \sum_{k=1}^{A} \langle i|\delta(\vec{r} - \vec{r}_k)|j\rangle \rho_{ji}. \tag{45}$$

Figures 1–6 present the equidensity contours of various HF and HFB solutions. All of these plots show the projection of the density distribution on a plane in which the axis of symmetry is the vertical axis. The densities are normalized with respect to the corresponding maximum density taken arbitrarily as unity.

In Fig. 1 we plot the contours of constant density for paired ^{32}S calculated with a space including only three oscillator shells. A similar plot but now including four oscillator shells is given in Fig. 2. Apart from the conspicuous increase in the over-all deformation, a comparison of the two figures reveals that the enhancement of pairing correlations is associated with a considerable shift of mass towards the center of the nucleus. The effect of pairing correlations on the nuclear shape and, in particular, the tendancy toward higher symmetry due to pairing is demonstrated in Figs. 3 and 4 by comparing the density distribution of the prolate HF solution and the prolate HFB solution for ^{24}Mg. In this case it can also be seen that there is an α-particle clustering in the HF solution, and that this effect is reduced in the HFB solution. A similar comparison is given for ^{36}Ar in Figs. 5 and 6 where we plot the density distributions for the oblate HF and HFB solutions.

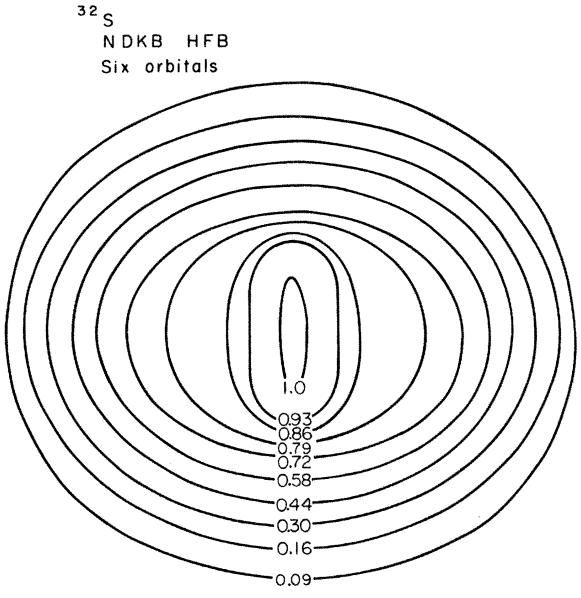

FIG. 1. Constant-density contour plot for the oblate HFB solution of ^{32}S within the space of s-p-s-d oscillator orbitals. The calculations were done for the NDKB or rms radius = 2.877 fm. The densities are given in units of 0.276 fm^{-3}.

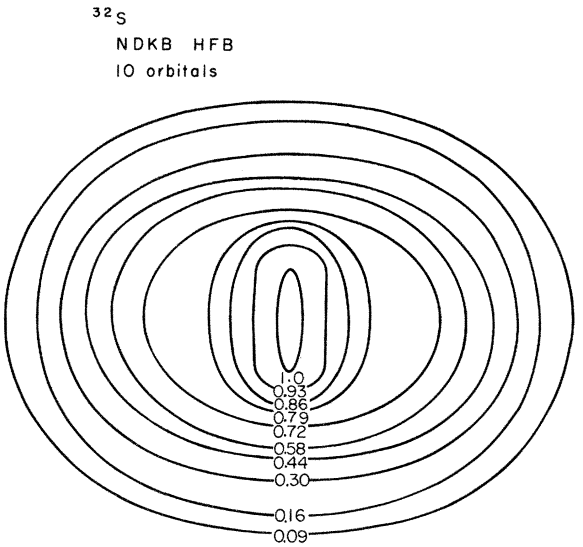

FIG. 2. Constant-density contour plot for the oblate HFB solution of ^{32}S within the space of s-p-s-d-p-f orbitals, again using the NDKB force. rms radius = 2.870 fm. The densities are given in units of 0.296 fm^{-3}.

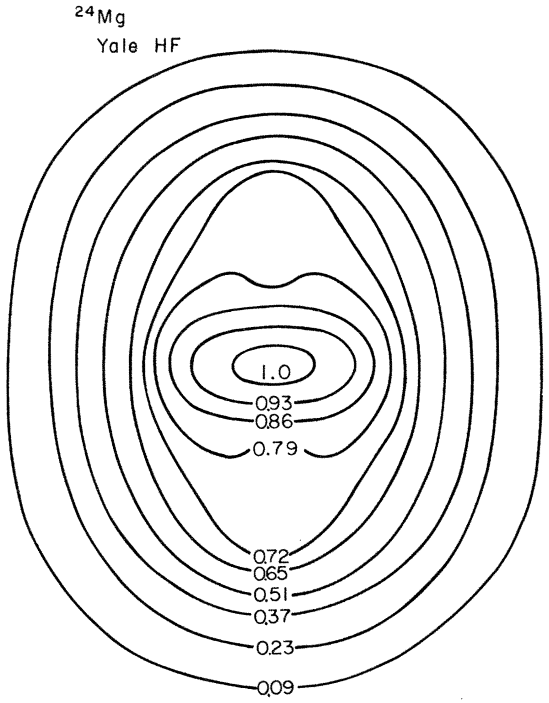

FIG. 3. Constant-density contour plot for the prolate HF solution of ^{24}Mg obtained with the Yale potential. rms radius = 2.853 fm. The densities are given in units of 0.240 fm^{-3}.

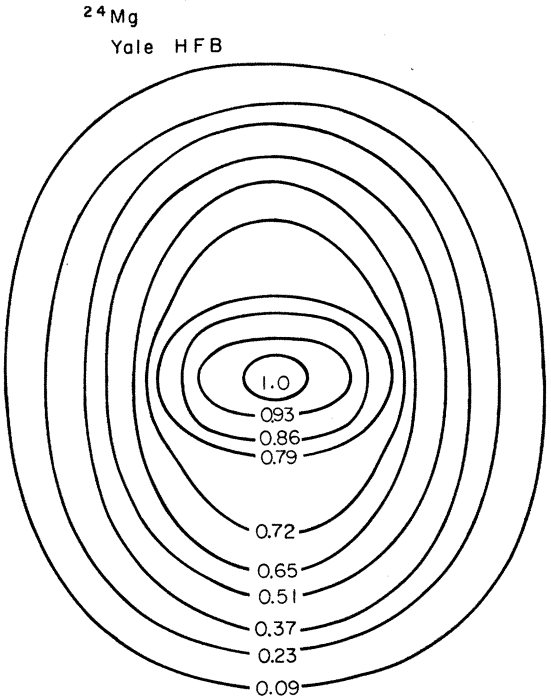

FIG. 4. Constant-density contour plot for the prolate HFB solution of ^{24}Mg obtained with the Yale potential. rms radius = 2.856 fm. The densities are given in units of 0.246 fm^{-3}.

Here again, a big reduction in deformation due to pairing is clearly demonstrated. It will be shown later that this reduction is responsible for correcting the discrepancy in the HF description for ^{36}Ar.

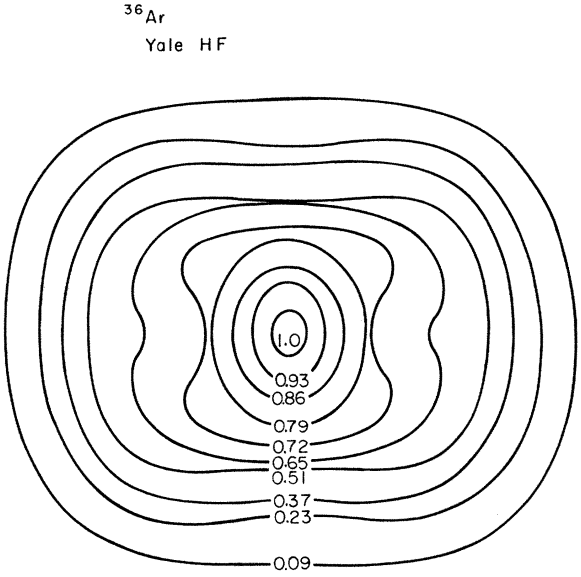

FIG. 5. Constant-density contour plot for the lowest oblate HF solution of ^{36}Ar obtained with the Yale force. rms radius = 3.017 fm. The densities are given in units of 0.302 fm^{-3}.

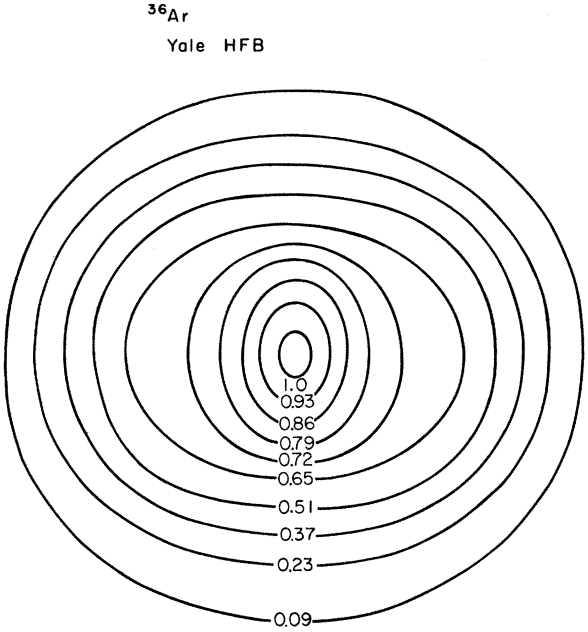

FIG. 6. Constant-density contour plot for the oblate HFB solution of ^{36}Ar obtained with the Yale potential. rms radius = 3.018 fm. The densities are given in units of 0.300 fm^{-3}.

The changes in shape of the HFB intrinsic states are also reflected in the total angular momentum contained in each state. It is interesting to compare the values of $\langle J^2 \rangle$ calculated with the wave functions given in Table I and the solutions with largest binding energy which are quoted in Ref. 22. When the values of $\langle J^2 \rangle$ are expressed in units of $\hbar^2$ a comparison shows ^{24}Mg(22.4 vs 24.4), ^{32}S(19.5 vs 25.4), and ^{36}Ar(13.0 vs 16.5). (The value from the HFB calculation appears first.) The decrease in angular momentum for the ^{24}Mg and ^{32}S HFB intrinsic states occurs because the HF solutions are triaxial and such nonsymmetric shapes contain large amounts of angular momentum.

Before we conclude this section we note that the inertial parameter A ($=\hbar^2/\hbar\mathcal{F}$ where $\mathcal{F}$ is the moment of inertia) is calculated using the Inglis cranking model.[25] The expression for the moment of inertia for an HFB intrinsic state is

$$\mathcal{F} = 2 \sum_{\substack{ij\mu \\ kl\nu \\ \sigma}} \frac{\langle i\mu|j_x|j\mu\rangle \langle k\nu|j_x|l\nu\rangle}{E_\sigma - E_0} v_{\alpha\rho,\, i\mu} u^*_{\alpha\rho,\, k\nu} \times v^*_{\beta\tau,\, l\nu} u_{\beta\tau,\, j\mu} . \quad (46)$$

In this expression, E_0 is the vacuum energy, E is the energy of a two-quasiparticle state ($E_\sigma = E_0 + E_{\alpha\rho} + E_{\beta\tau}$), and the sum on σ is made in such a way as to avoid double counting the two-quasiparticle states. On observing the structure of (46), one might expect that since the gaps increase in HFB over the values obtained from the HF + BCS approximation, that the inertial parameters will be somewhat larger. The limitations of the cranking model have been discussed in I.

V. COMPARISON WITH EXPERIMENT

It was pointed out in Sec. III that the HFB solutions with the largest binding energy exhibit only $T = 0$ pairing. This was also a feature of the calculations in I, and the reasons for this phenomenon are discussed there. Another general feature of the HFB solutions is the near degeneracy (in $\langle H \rangle$) of several solutions. These solutions have a large overlap, and so only one of them is physically relevant as far as the low-energy spectrum is concerned. Self-consistent field calculations are usually unable to make the proper choice among these nearly degenerate solutions because of the neglect of many higher-order corrections (see discussion in I). Nevertheless, it is often possible to compare properties predicted by the various intrinsic states with experimental information, and eliminate the nonphysical states. Below, we will consider the nuclei individually.

^{20}Ne. The ground intrinsic state is adequately described by a prolate HF solution.[26] For this solution, pairing corrections are small[27] and can not be calculated by our methods (see discussion in I).

^{24}Mg. HF theory predicts[28] the ground-state shape to be triaxial (in agreement with SU_3 theory[29]). In I we discussed in detail experimental evidence which shows that this nucleus is best described by an axial prolate intrinsic state.[30,31] Since that time an exact projection of angular momentum has been carried out[32] which shows that this intrinsic state does not produce an $I(I+1)$ spectrum for either the $K = 0$ or $K = 2$ bands, a feature which is in sharp contradiction to experiment. Further, the $K = 0$ and $K = 2$ band splitting is underestimated by 1.7 MeV. With Yale-Shakin t-matrix elements, the HFB equations give almost degenerate solutions: (1) the triaxial HF state with $\langle H \rangle = -133.14$ MeV, (2) a prolate paired state with $\langle H \rangle = -132.53$ MeV, and (3) an oblate paired state where $\langle H \rangle = -132.05$ MeV. The HF intrinsic state is incompatible with experiment. Recently, the quadrupole moment of the first 2+ state of ^{24}Mg has been measured,[33] and is found to have a negative sign consistent with a prolate shape for the intrinsic state. This rules out the axial oblate solution. The axially symmetric prolate solution seems to be consistent with experimental data. It trivially gives the $I(I+1)$ spectra for the $K = 0$ and $K = 2$ bands. The cranking value of the inertial parameter for the ground band is found to be 0.33 MeV, and the unperturbed position of the lowest $K = 2+$ two-quasiparticle state is 4.81 MeV. The paired prolate intrinsic state gives a much more consistent description of experimental data than any HF state.

^{28}Si. It is well known that HF predicts two nearly degenerate and orthogonal solutions, one being axially symmetric prolate, and the other oblate. The ordering of the two states, based on the value of $\langle H \rangle$, depends on the particular force used.[22,34] Experimentally, one does not see two low-lying $K = 0$ bands, and it has been theoretically shown that the bands can not be separated by mixing.[35] Furthermore, recent experimental measurements[36] of the quadrupole moment of the first 2+ state show that the band is in fact oblate. But the ground-state band deviates considerably from an $I(I+1)$ spectrum, since the $J = 0$ member of the band is too low. It has recently been suggested[37] that this depression could be explained by the interaction of the $J = 0$ member with a coexisting spherical state. However HF calculations with realistic forces predict a spherical state that is much too high to be associated with the coexisting spherical state seen at 4.98 MeV. Unfortunately the solutions to the HFB equations also give force-dependent results. The Yale t matrix gives identical results to HF, because both the prolate and oblate HF solution have single-particle gaps that are too large to permit pairing correlations using our methods. However, with the NDKB potential, we find an isospin-paired axially symmetric prolate solution almost degenerate with the prolate and oblate HF solutions. This HFB prolate solution has a significant overlap with both the HF solutions, since all the single-particle states are partially occupied because of the pairing correlations. With this potential, one can discard the prolate HF solution because of its small energy gap, and the prolate HFB solution because of its large overlap with the oblate HF solution. The latter solution appears to be in essential agreement with experiment if the coexistence picture is accepted. However, we are unable to produce a low-energy spherical solution with any of the potentials used.

^{32}S. HF theory predicts a triaxial intrinsic shape for ^{32}S. This state is very peculiar, since the inertial parameters about all three axes are equal, and it has a vanishing quadrupole distortion parameter.[7] Physical predictions made from this

intrinsic state do not agree with experiment. However, it is possible to interpret the experimental data using an axially symmetric intrinsic state if one considers coexistence[37] of a spherical intrinsic state which appears at 3.78 MeV. The solutions to the HFB equations again give three solutions with similar binding energies. With the Yale t matrix we find the triaxial HFB solution with $\langle H\rangle = -227.74$ MeV, a paired axially symmetric oblate state with $\langle H\rangle = -229.66$ MeV, and a paired axially symmetric prolate state with $\langle H\rangle = 224.53$ MeV. All three solutions have significant overlap and only one can be an acceptable intrinsic state. The asymmetric state can be eliminated since it disagrees with the experimental data. However, since there has been no experimental measure of the quadrupole moment of the first 2+ state, we can not choose between the oblate and prolate axially symmetric solutions. As in the case of ^{28}Si we were not able to find a spherical solution with a sufficiently low energy to be the coexisting state.

^{36}Ar. This nucleus is very interesting because phenomenologically one can interpret the low-lying spectrum as being vibrational. On the other hand, HF calculations give a deformed oblate state ($\langle H\rangle = -291.07$ MeV for the Yale t matrix) with a large energy gap and a small value for the inertial parameter. This intrinsic state of course predicts low-lying rotational structure which is in disagreement with experiment. The solutions to the HFB equations offer a possible answer to the problem. One obtains a paired oblate solution lower in energy than the HF solution ($\langle H\rangle = -291.77$ MeV). This HFB solution is remarkable in that its inertial parameter is unusually large ($A = 0.62$). This means that the rotational states appear at energies comparable with the two-quasiparticle states which results in the destruction of the rotational structure.

A recent paper by de Swiniarski *et al.*[38] has used a coupled-channel analysis of inelastic scattering data to determine the β_2 and β_4 values for the $N = Z$ even-even nuclei. In Fig. 7 we compare our calculated values with the results of their analysis. The theoretical numbers are calculated with the wave functions in Table II for ^{24}Mg, ^{32}S, and ^{36}Ar. We use the wave functions from Ref. 21 for ^{20}Ne and ^{28}Si. In Fig. 8 we compare the inertial parameters calculated with these wave functions with the values obtained from experiment, as discussed in I. We also plot the HF results. A comparison of Fig. 2 in I and Fig. 8 shows that the inertial parameter increases in HFB over the HF + BCS approximation by 20%. As pointed out in Sec. IV, this is caused by the increase in the gap.

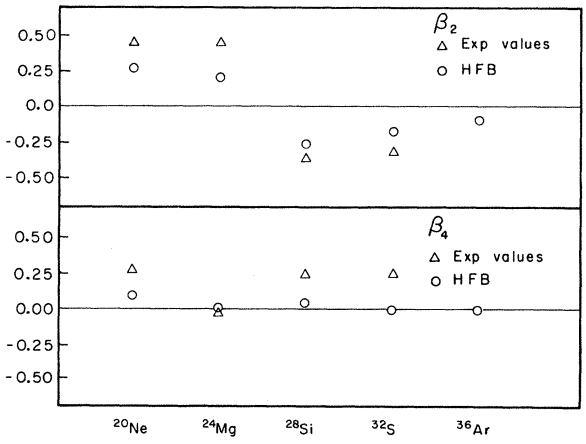

FIG. 7. The calculated values of distortion parameters β_2 and β_4 are compared with the experimental values of de Swiniarski *et al.* (See Ref. 38.) For ^{20}Ne and ^{28}Si the theoretical value corresponds to the HF value.

VI. CONCLUSION

In previous work[6,10] we have investigated the existence of generalized isospin ($T = 0$ and $T = 1$) pairing with the assumption that the pair potential is diagonal in space-spin coordinates. The HFB equations have now been solved without making this approximation and also using "realistic force." All approximations to the HFB equations (HF and BCS, iterating between HF and BCS, and HB + BCS) have serious defects. They fail to approximate the exact (HFB) wave functions. The first two approximations underestimate the pairing energy (often by a factor of 2 or 3). The HFB canonical single-particle basis often bears no similarity to the HF single-particle basis.

The third transformation of the Bloch-Messiah theorem may not be approximated by the unit matrix, nor is the pair potential diagonal in the canonical basis.

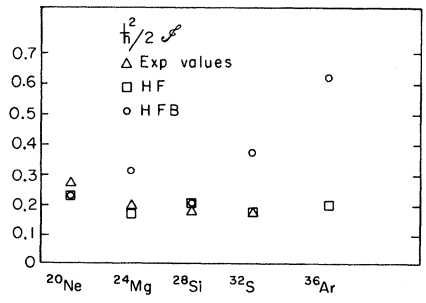

FIG. 8. The theoretical value of the moment-of-inertia parameter $\hbar/2\mathcal{I}$ (in MeV) are compared with the experimental values. For ^{28}Si and ^{32}S, the experimental values given are as extracted in Ref. 37. For ^{20}Ne and ^{28}Si the HFB value corresponds to the HF value.

Iterating between the HF and the BCS equations in an attempt to permit both degrees of freedom to interact with one another[6] results in an even worse approximation to HFB than merely solving the BCS equations with the trivial HF basis but allowing HF single-particle energies to be modified by pairing. Presumably this results from the lack of self-consistency in the former method. To permit both $T=0$ and $T=1$ pairing it is necessary to use complex quasiparticle coordinates. In practice, however, $T=0$ pairing always suppresses $T=1$ pairing.

Nevertheless, the results regarding the equilibrium shapes remain much the same as in I: $T=0$ pairing produces an intrinsic state which is axially symmetric for ^{24}Mg and ^{32}S. These paired solutions are likely to be closer to the physical intrinsic state on the basis of comparison with experiment. $T=0$ pairing also provides an explanation for the lack of rotational structure in ^{36}Ar. We conclude that isospin ($T=0$) pairing is an important correlation effect for light nuclei. As far as we know, this is the only occasion that pairing occurs in nature in other than singlet S states. Furthermore, the isospin-pairing phenomenon is distinguished by the largeness of the pairing energy. Much work, theoretical and experimental, remains to be done before a complete understanding of this phenomenon of isospin pairing is achieved.

ACKNOWLEDGMENTS

The authors wish to thank Dr. P. Sauer, Dr. S. N. Tewari, and H. Wolter for useful discussion. They particularly wish to thank H. Wolter for help in calculating the inertial parameters. The authors also wish to acknowledge the help of P. S. Rajasekhar in calculating two-body matrix elements. One of us (J. B.) wishes to thank Dr. N. K. Glendenning and the Division of Nuclear Chemistry of the Lawrence Radiation Laboratory for their kind hospitality during the summer of 1969.

---

*Work performed under the auspices of the U. S. Atomic Energy Commission.

†Present address: Argonne National Laboratory, Argonne, Illinois.

[1]D. L. Hill and J. A. Wheeler, Phys. Rev. 89, 1106 (1953).

[2]See for example, A. Bohr and B. R. Mottelson, to be published.

[3]S. G. Nilsson, Kgl. Danske Videnskab. Selskab, Mat.-Fys. Medd. 29, No. 16 (1955).

[4]G. Ripka, in *Lectures in Theoretical Physics,* edited by W. E. Brittin *et al.* (University of Colorado Press, Boulder, Colorado, 1965).

[5]G. Ripka, in *Advances in Nuclear Physics,* edited by M. Baranger and E. Vogt (Plenum Press, Inc., New York, 1968), Vol. I.

[6]J. Bar-Touv, A. Goswami, A. L. Goodman, and G. L. Struble, Phys. Rev. 178, 1670 (1969).

[7]M. K. Banergee, C. A. Levinson, and G. J. Stephenson, Jr., Phys. Rev. 178, 1709 (1969).

[8]L. Satpathy, D. Goss, and M. K. Banerjee, Phys. Rev. 183, 887 (1969).

[9]P. Sauer, A. Faessler, and H. Wolter, Nucl. Phys. A125, 257 (1969).

[10]A. L. Goodman, G. L. Struble, and A. Goswami, Phys. Letters 26, B260 (1968).

[11]M. Baranger and K. Kumar, Nucl. Phys. A92, 608 (1967).

[12]C. Bloch, Lecture Notes, Tata Institute, Bombay, 1962 (unpublished).

[13]P. U. Sauer, Nuovo Cimento 57B, 62 (1968).

[14]See for example, Refs. 7 and 8.

[15]H. T. Chen and A. Goswami, Phys. Letters 24, B257 (1967).

[16]A. Goswami and L. S. Kisslinger, Phys. Rev. 140, B26 (1965).

[17]C. Bloch and A. Messiah, Nucl. Phys. 39, 95 (1962).

[18]A. L. Goodman, Ph.D. thesis, University of California, Lawrence Radiation Laboratory, 1969 (unpublished).

[19]K. Dietrich, H. T. Mang, and J. Pradhal, Z. Physik 190, 357 (1966).

[20]K. E. Lassila, M. H. Hull, Jr., H. M. Ruppel, F. A. McDonald, and G. Breit, Phys. Rev. 128, 881 (1962).

[21]C. M. Shakin, Y. R. Waghmare, and M. H. Hull, Phys. Rev. 161, 1006 (1967).

[22]M. K. Pal and A. P. Stamp. Phys. Rev. 158, 924 (1967).

[23]C. W. Nestor, K. T. R. Davis, S. J. Krieger, and M. Baranger, Nucl. Phys. A113, 14 (1968).

[24]J. Bar-Touv and I. Kelson, Phys. Rev. 138, B1035 (1965).

[25]D. R. Inglis, Phys. Rev. 96, 1059 (1954); *ibid.* 97, 1701 (1955).

[26]S. N. Tewari, Phys. Letters 29B, 5 (1969).

[27]M. K. Pal and A. P. Stamp, Nucl. Phys. A99, 228 (1967).

[28]First pointed out in Ref. 24.

[29]For the most recent SU_3 based shell-model calculation see A. Arima *et al.*, Nucl. Phys. A138, 273 (1969).

[30]J. C. Parikh, Phys. Letters 26, B607 (1968).

[31]B. Cujec, Phys. Rev. 136, B1305 (1969); G. J. McCallum and B. J. Schwerby, Phys. Letters 25, B109 (1967).

[32]B. Giraud and P. U. Sauer, in *Proceedings of the International Conference on Properties of Nuclear States, Montreal, Canada, 1969,* edited by M. Harvey *et al.* (Presses de l'Université de Montréal, Montréal, Canada, 1969).

[33]O. Hausser, T. K. Alexander, D. Pelte, B. W. Hooton, and H. C. Evans, Phys. Rev. Letters 22, 359 (1969).

[34]S. DasGupta and M. Harvey, Nucl. Phys. A94, 602 (1967).

[35]S. N. Tewari and D. Grillot, Phys. Rev. 177, 1717 (1969).
[36]O. Hausser, T. K. Alexander, D. Pelte, B. W. Hooton, and H. C. Evans, Phys. Rev. Letters 23, 320 (1969).
[37]J. Bar-Touv and A. Goswami, Phys. Letters 28, B391 (1968).
[38]R. de Swiniarski, C. Glashausser, D. L. Hendrie, J. Sherman, A. D. Bacher, and E. A. McClatchie, Phys. Rev. Letters 23, 317 (1969).

PHYSICAL REVIEW C VOLUME 2, NUMBER 2 AUGUST 1970

Level Structure of ^{17}O and the ^{13}C(^{6}Li,d) and ^{13}C(^{7}Li,t) Reactions*

K. Bethge,† D. J. Pullen, and R. Middleton
Physics Department, University of Pennsylvania, Philadelphia, Pennsylvania 19104
(Received 16 April 1970)

The reactions ^{13}C(^{7}Li,t)^{17}O and ^{13}C(^{6}Li,d)^{17}O have been studied at 17 and 18 MeV, respectively. Both reactions are selective in the states they populate, although this is more evident in the (^{7}Li,t) case. Angular distributions were extracted for 15 levels below 8.5-MeV excitation. These exhibit pronounced structures and are generally indicative of direct-reaction mechanisms. Transitions to the negative-parity states at 3.06, 3.85, and 4.55 MeV are the strongest observed below 7-MeV excitation. These levels are discussed within the framework of the weak-coupling model and the transitions compared with those from the ^{12}C(^{7}Li,t) and ^{12}C(^{6}Li,d) reactions leading to the first $K=0$ rotational band in ^{16}O. Strong transitions are also observed to levels at 7.38, (8.46, 8.49), (8.87, 8.95), and (9.14, 9.20) MeV.

I. INTRODUCTION

The level structure of ^{17}O has been the subject of many experimental and theoretical studies.[1-12] The simple shell model which treats the ^{16}O core as inert is unable to account for the low-lying negative-parity states or the multiplicity of positive-parity states which lie just above 5-MeV excitation. These states originate from excitations of the core and a number of calculations have been performed for ^{17}O within the framework of an excited-core model.[8-12]

In order to investigate the particle-hole configurations of ^{17}O, it is convenient to employ transfer reactions in which the "hole" component is already present in the target nucleus. In this respect, ^{6,7}Li-induced reactions offer a convenient means for studying ^{17}O. In particular, recent studies[13,14] of the α-transfer reactions (^{6}Li, d) and (^{7}Li, t) with nuclei in the $2s$-$1d$ shell have shown them to be rather selective in the states they populate and that a direct-reaction mechanism plays an important role. It was therefore of interest to determine whether the ^{13}C(^{6}Li, d) and ^{13}C(^{7}Li, t) reactions would also show similar selectivity, and in particular it was hoped that the negative-parity states in ^{17}O having predominantly 4p-3h configurations could be identified. For purposes of comparison, the latter also prompted a study of the ^{12}C(^{6}Li, d) and ^{12}C(^{7}Li, t) reactions leading to the first $K=0$ rotational band in ^{16}O.

II. EXPERIMENTAL TECHNIQUES AND RESULTS

The ^{13}C(^{6}Li, d) and ^{13}C(^{7}Li, t) reactions were studied using 18-MeV ^{6}Li-ions and 17-MeV ^{7}Li-ions from the University of Pennsylvania tandem accelerator. Self-supporting ^{13}C targets were employed with 60 ± 14 μg/cm^2 thickness, as determined from a differential weighing measurement. The deuterons and tritons were momentum-analyzed in a multiangle spectrograph over an angular range $3\frac{3}{4}$ to $172\frac{1}{2}°$ and detected in nuclear emulsions. The angular interval with which distributions could be measured in a single exposure was $7\frac{1}{2}°$. However, by rotating the spectrograph through $3\frac{3}{4}°$ and performing two exposures for each reaction, angular distributions were obtained in $3\frac{3}{4}°$ intervals.

A deuteron spectrum measured at 30° and a triton spectrum at $7\frac{1}{2}°$ are shown in Fig. 1. The overall energy resolutions (full width at half maximum) were 60 and 85 keV for the (^{6}Li, d) and (^{7}Li, t) studies, respectively, determined mainly by the target thicknesses. Groups corresponding to states in ^{17}O are indicated by their corresponding excitation energies and those to states in ^{16}O are shown cross hatched. The latter arise from ^{12}C impurity in the ^{13}C targets, and from carbon buildup during the exposures. The relative strengths of groups $^{16}O_6$ and $^{16}O_7$, indicated by the broken lines in the spectra, were determined from a separate study of the (^{6}Li, d) and (^{7}Li, t) reactions on ^{12}C (see below).